Supporting Information

All-acrylic film-forming colloidal polymer/silica nanocomposite particles prepared by aqueous emulsion polymerization

Lee A. Fielding, Jeff Tonnar and Steven P. Armes*

Figure S1. FT-IR spectra recorded for freeze-dried poly(methyl methacrylate-co-n-butyl acrylate)/silica nanocomposite particles with varying comonomer ratios. The C-H bands at 2995 and 2841 cm^{-1} due to methyl methacrylate residues become less prominent, while the band at 2874 cm^{-1} attributed to the C-H stretch of the n-butyl acrylate residues gradually becomes more intense.

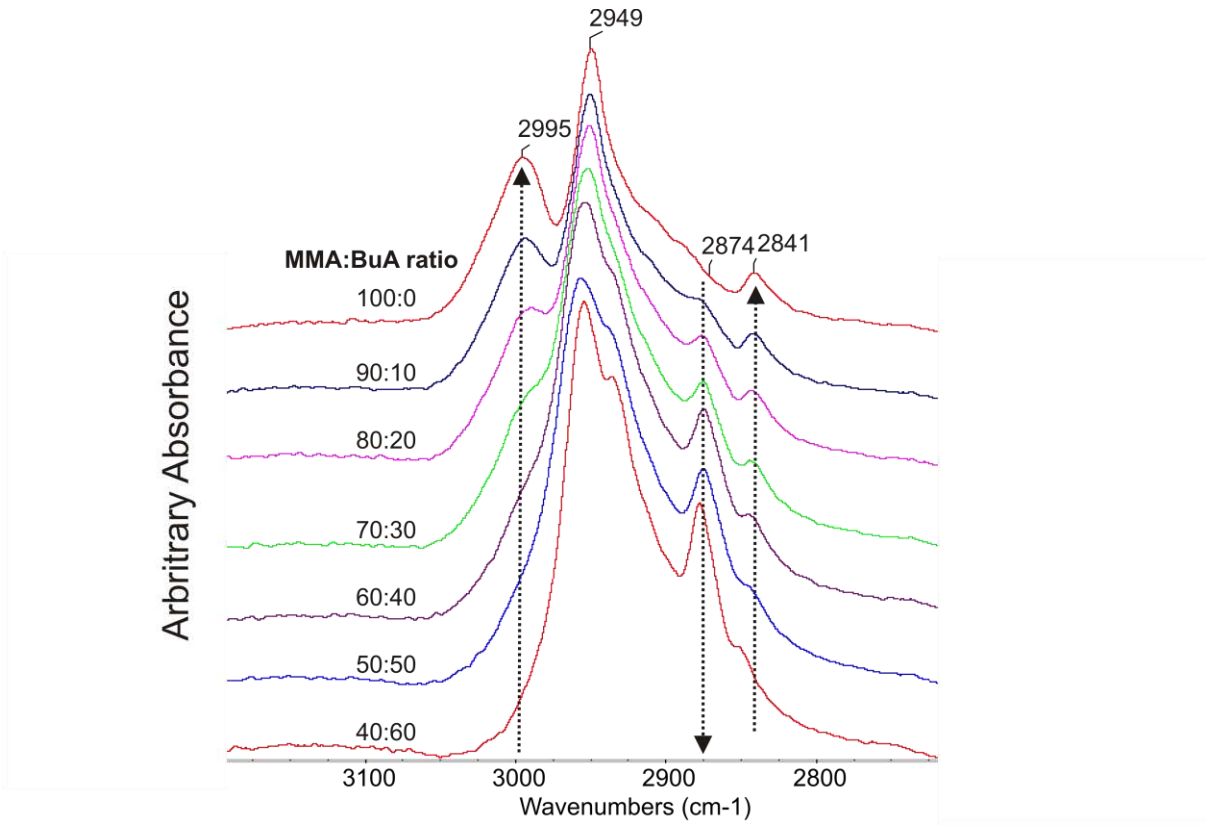

Figure S2. ^{1}H NMR spectra of poly(methyl methacrylate-co-n-butyl acrylate)/silica nanocomposite particles prepared with varying comonomer ratios. With increasing n-butyl acrylate content the OCH_2 signal at 3.80-4.20 ppm increases, whereas the OCH_3 signal at 3.50-3.75 ppm due to methyl methacrylate residues is reduced. The copolymer/silica particles were freeze-dried and the organic component dissolved in $CDCl_3$ prior to NMR analysis.

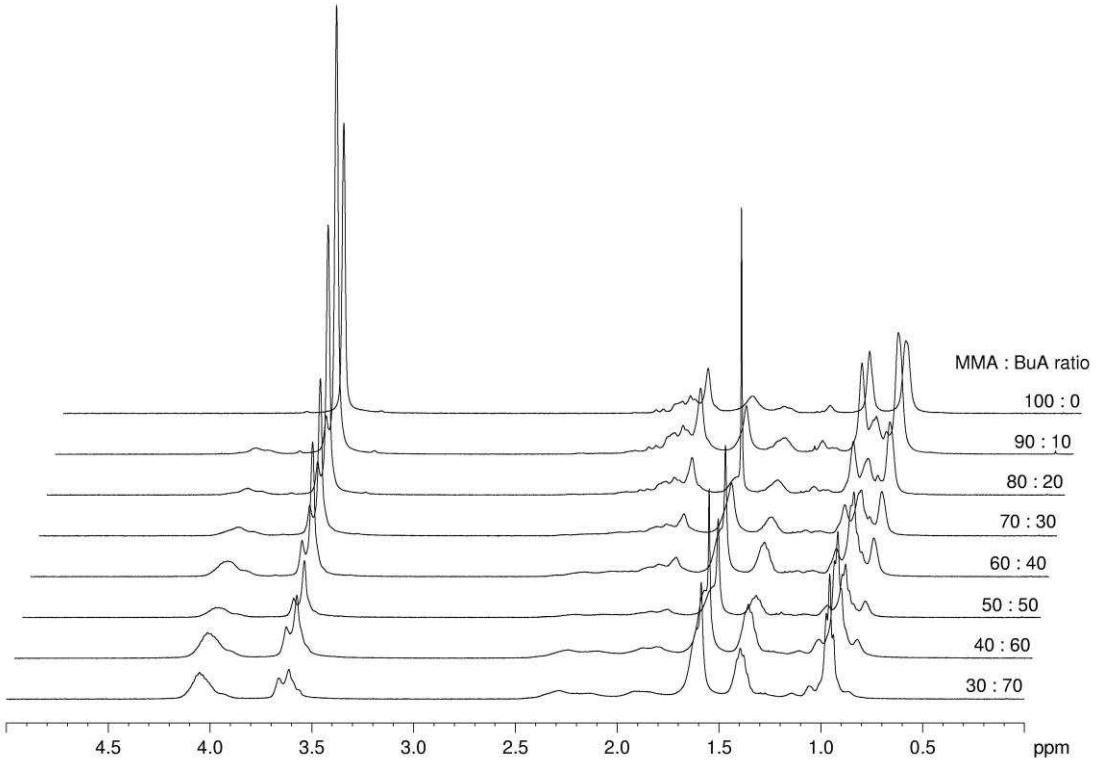

Table S1. Copolymer compositions for various poly(methyl methacrylate-co-n-butyl acrylate)/silica nanocomposite particles determined using ^{1}H NMR spectroscopy.

Targeted MMA : BuA weight ratio[a]	Calculated MMA : BuA molar ratio[b]	Calculated MMA : BuA weight ratio[b]
100 : 0	100 : 0	100 : 0
90 : 10	91 : 9	89 : 11
80 : 20	86 : 14	83 : 17
70 : 30	76 : 24	72 : 28
60 : 40	64 : 36	58 : 42
50 : 50	60 : 40	54 : 46
40 : 60	47 : 53	40 : 60
30 : 70	36 : 64	30 : 70

[a] Comonomer ratio targeted in nanocomposite particle synthesis. [b] Calculated molar and weight ratios determined from integration of ^{1}H NMR signal at 3.6 and 4.1 for MMA and BuA respectively.

Figure S3. XPS survey spectra recorded for various freeze-dried poly(methyl methacrylate-co-n-butyl acrylate)/silica nanocomposite particles. The poly(methyl methacrylate)/silica nanocomposite corresponds to entry 18 in Table 1 and the copolymer/silica nanocomposites correspond to entries 1-6 in Table 2. The freeze-dried powders were pressed onto indium foil prior to analysis.

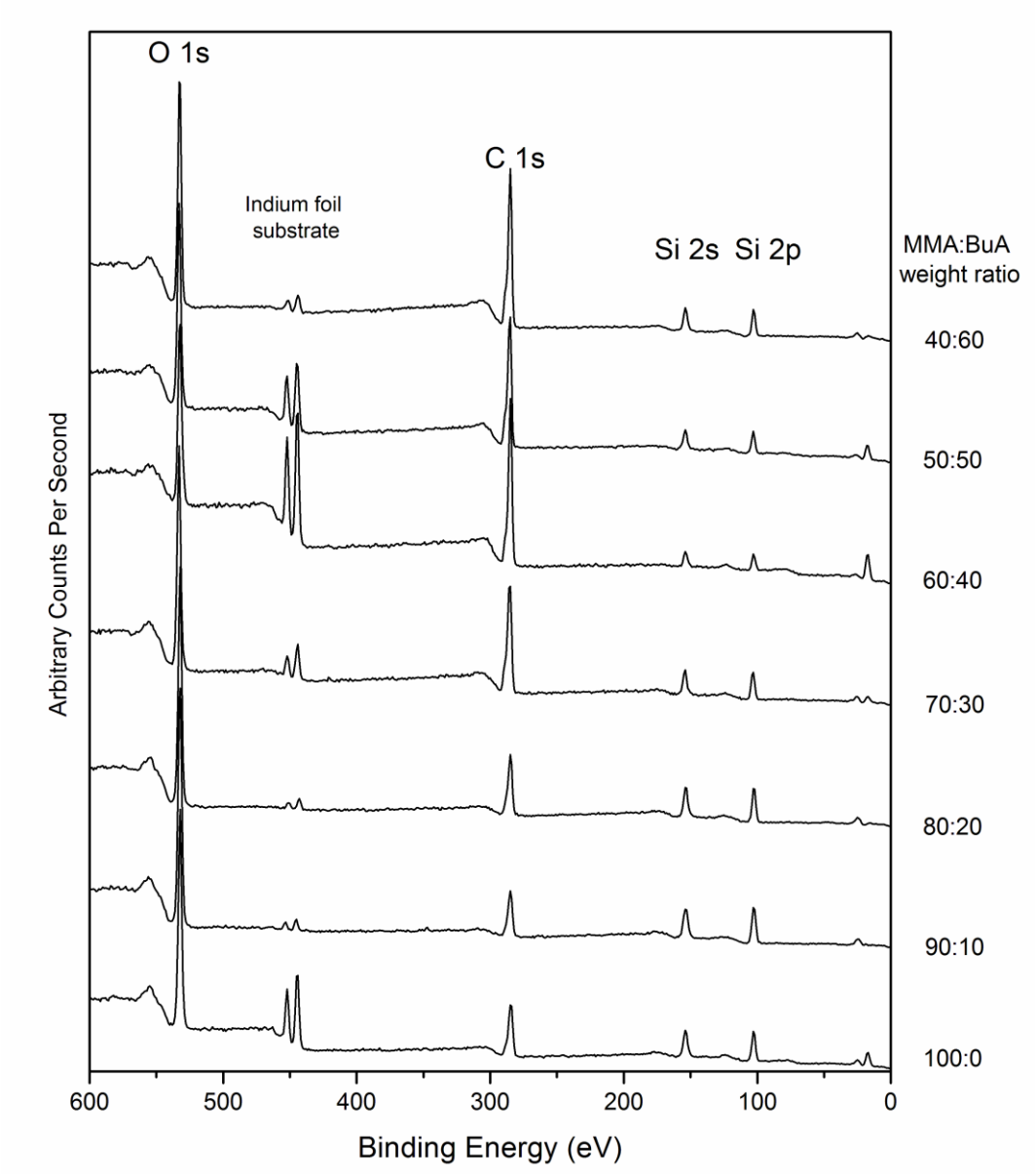

Figure S4. Digital photographs of a 40:60 P(MMA-BuA)/silica nanocomposite film (A) prior to deformation, (B-E) deformation of the film by bending in various directions and (F) after manipulation. Thus such nanocomposite films are highly flexible and remain transparent throughout manipulation.

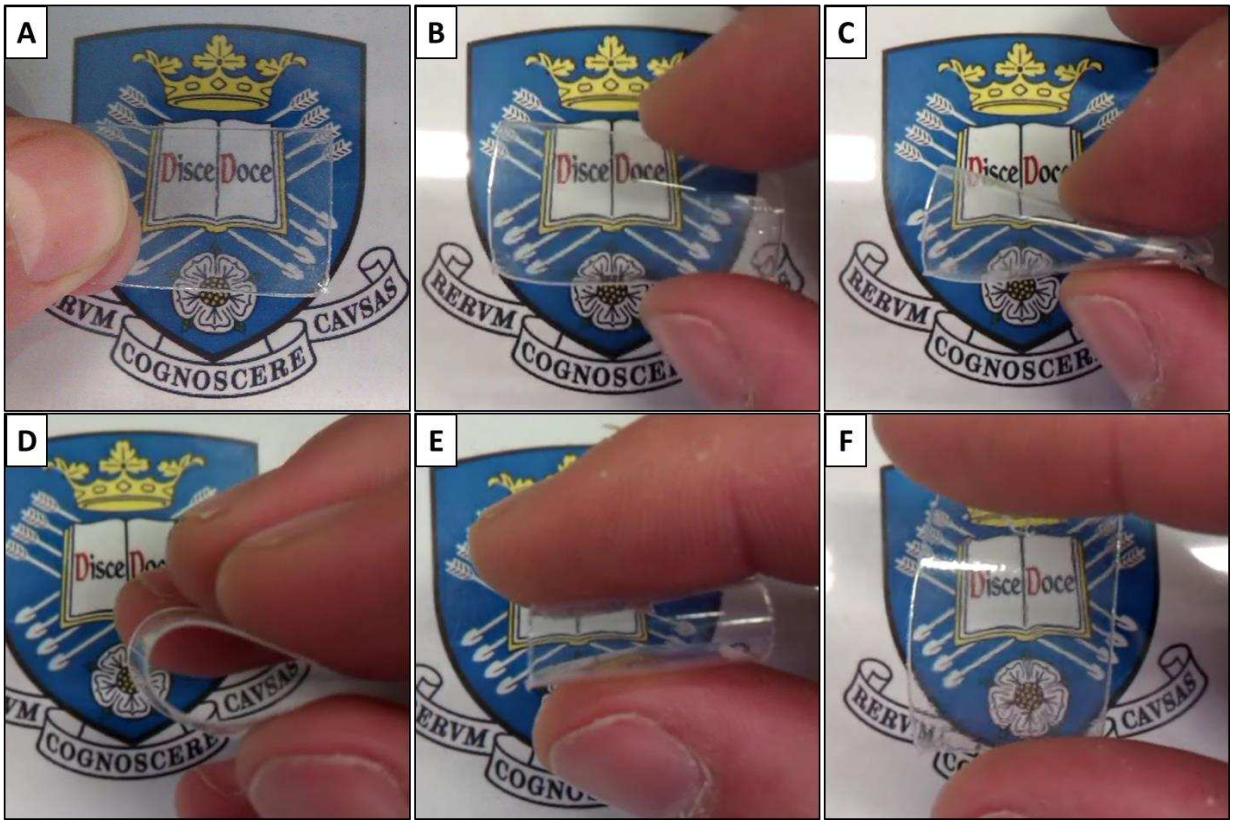

Figure S5. UV-visible absorption spectra recorded in transmission mode for a 50:50 poly(methyl methacrylate-co-n-butyl methacrylate)/silica film (entry 5 in Table 2) and the corresponding 50:50 poly(methyl methacrylate-co-n-butyl methacrylate) copolymer latex film prepared using ammonium persulfate initiator and sodium n-dodecyl sulfate (1.0 wt.% surfactant based on monomer). Each film had a mean thickness of approximately 250 µm.

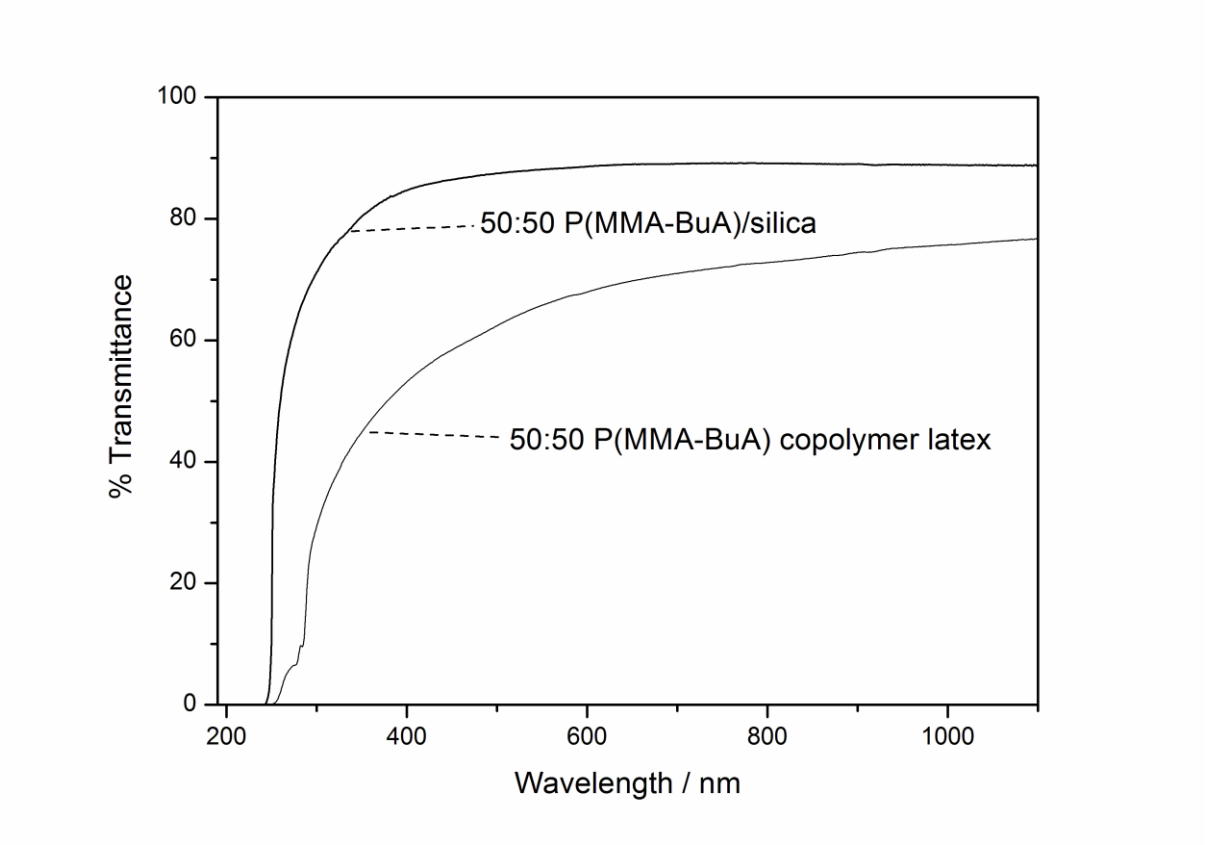

Figure S6. Weight-average particle size distributions for poly(methyl methacrylate)/silica nanocomposite particles (a) formed when insufficient silica (scaled up version of entry 11 in Table 1) is present during homopolymerization and (b) after sonication of this flocculated nanocomposite dispersion. Known amounts of silica sol [(c) 5 wt. %, (d) 27 wt. % or (e) 53 wt. % based on the mass of nanocomposite particles] were then added to this flocculated dispersion, followed by sonication and DCP analysis to examine whether a higher degree of dispersion had been achieved.